Probing the Superfluid Velocity with a Superconducting Tip: The Doppler Shift Effect

A. Kohen,[1] Th. Proslier,[1] T. Cren,[1] Y. Noat,[1] W. Sacks,[1] H. Berger,[2] and D. Roditchev[1]

[1]*Institut des Nanosciences de Paris, I.N.S.P., Universités Paris 6 et 7, C.N.R.S. (UMR 75 88), 75015 Paris, France*

[2]*Institute of Physics of Complex Matter, E.P.F.L., 1015 Lausanne, Switzerland*

(Received 28 November 2005; published 14 July 2006)

We address the question of probing the supercurrents in superconducting (SC) samples on a local scale by performing scanning tunneling spectroscopy (STS) experiments with a SC tip. In this configuration, we show that the tunneling conductance is highly sensitive to the Doppler shift term in the SC quasiparticle (QP) spectrum of the sample, thus allowing the local study of the superfluid velocity. Intrinsic screening currents, such as those surrounding the vortex cores in a type II SC in a magnetic field, are directly probed. With Nb tips, the STS mapping of the vortices, in single crystal $2H$-$NbSe_2$, reveals *both* the vortex cores, on the scale of the SC coherence length ξ, *and* the supercurrents, on the scale of the London penetration length λ. A subtle interplay between the SC pair potential and the supercurrents at the vortex edge is observed. Our results open interesting prospects for the study of screening currents in any superconductor.

DOI: 10.1103/PhysRevLett.97.027001 PACS numbers: 74.25.Ha, 07.79.Cz, 74.25.Jb, 74.50.+r

A fundamental property of the superconducting (SC) state is its response to a magnetic field. In particular, the field penetrates type II superconductors in the form of quantized flux, or vortices, each one carrying a flux quantum $\phi_0 = h/2e$, which are arranged in a lattice [1]. Each vortex is surrounded by screening currents decaying over λ, the magnetic penetration length, and has a core extending over the coherence length ξ. The SC pair potential (PP), $\Delta(\mathbf{r})$, decays from its maximal value outside the core, down to zero in its center. As shown by Bardeen, Cooper, Schrieffer (BCS), in the spatially homogenous case the SC state has an excitation spectrum given by $E_{\mathbf{k}} = (\varepsilon_{\mathbf{k}}^2 + \Delta^2)^{1/2}$. This results in a unique quasiparticle (QP) density of states (DOS) in which a gap of width Δ, with a peak at its edge, opens at the Fermi level. In the vortex state, the DOS in the SC becomes spatially inhomogeneous due to both the currents flowing around the vortices and the variations in $\Delta(\mathbf{r})$. The two different effects are expected to occur on the length scales λ and ξ, respectively. As can be seen from the BCS spectrum, changing $\Delta(\mathbf{r})$ would modify the DOS gap width. In addition, as shown by Caroli *et al.* [2], bound states are formed in the vortex core since $\Delta(\mathbf{r})$ acts as a potential well. The bound states affect the low energy DOS and are significant close to the vortex center.

The scanning tunneling microscope (STM) is an instrument of choice to map the DOS variations on a nanometer scale. The technique is based on the tunneling current (I), flowing between a normal metal tip and a sample, measured as a function of the tip position and the bias voltage (V). Combined with spectroscopy (STS), the conductance $dI/dV(\mathbf{r}, V)$ reflects the sample local DOS, which has been exploited to study the vortex lattice [3–6]. The main focus of these experiments was a detailed study of the vortex core bound states and/or the measurement of ξ, as inferred from the spectra due to the spatial variation of $\Delta(\mathbf{r})$. Study of the screening currents, and thus measuring λ, had proven to be more delicate.

In general, when a uniform current flows in a SC sample, the excitation spectrum can be rewritten as:

$$E_{\mathbf{k}} = (\varepsilon_{\mathbf{k}}^2 + \Delta^2)^{1/2} + m\mathbf{v_F} \cdot \mathbf{v_s} \quad (1)$$

where $\mathbf{v_F}$ is the Fermi velocity and $\mathbf{v_s}$ is the superfluid one [7]. As long as the Doppler energy $m\mathbf{v_F} \cdot \mathbf{v_s}$ is small with respect to Δ, the main effect on the DOS is a reduction in the peak height. Recently, this was indeed observed in low resistance planar junctions at ultralow temperatures [8]. However, in STM it results in a relatively small effect, only a few percent, and is not effective as a means to study the supercurrents. Other scanning methods, such as Hall probe or SQUID microscopies [9] measure the local magnetic field and not the supercurrents. While allowing us to estimate λ, they lack the high spatial resolution of STM and are completely insensitive to $\Delta(\mathbf{r})$ and thus cannot be used to determine ξ. Recently the effect of an applied current on the zero bias conductance peak in d-wave superconductors was measured by STM [10].

The pioneering STS experiments of Hess *et al.* [3] have imaged the vortex core and bound states in $NbSe_2$. Additionally [4] they have attempted to extract the Doppler energy from the shift in the voltage position of a small shoulder appearing at low energy in their tunneling spectra. Theoretically it was shown in [11] that the Doppler shift model does not hold when the core states are significant, i.e., close to the vortex core and at low energy. This could explain why the approach of [4], while being qualitatively correct, failed to be quantative.

Here we take a different approach and use a SC tip, in STM/STS, to detect the pair supercurrents, due to their Doppler shift effect on a high energy feature: the peak in the SIS (SC-vacuum-SC) QP spectrum. The use of SC tips in STM was already shown [12–16]; however, no spectroscopy mapping in the mixed state was reported. *A priori*, their use to image the vortex lattice could result in complications. First, the local magnetic field might affect the tip's SC properties and second, the force acting between

the diamagnetic SC tip and the vortices might displace the vortices and distort the STS images. In this Letter we report the successful use of SC Nb tips for STS mapping of the vortex lattice in $NbSe_2$. Owing to the enhanced spectroscopic resolution of the SC tip, we detect *both* the in-core bound states and the supercurrents flowing around the vortices. The latter is achieved by the strong effect of the Doppler shift on the gap-edge peak amplitude.

The expected effect of supercurrents on a normal metal/insulator/superconductor (NIS) spectrum, as calculated using BCS, is shown in Fig. 1(a). One sees that for $m\mathbf{v_F} \cdot \mathbf{v_s} < \Delta$ the corresponding change in the conductance spectrum is very small and thus is difficult to observe experimentally. However, in the SIS geometry [Fig. 1(b)] the same changes in the sample DOS, due to the Doppler shift, significantly change the amplitude of the conductance peak and slightly broaden it, see Fig. 1(b). The enhancement of the changes in the peak height is due to the overlap of the tip and sample DOS gap edges. Closer to the vortex core, the main change of the QP DOS should be the decrease in the magnitude of Δ, manifested by a gradual shift of the conductance peaks towards lower energies, see Fig. 1(c). Thus, in the SIS configuration, one expects two different behaviors in the SIS conductance spectra while approaching the vortex core: a decrease in the peak *amplitude* at large distances and a peak *shift* to lower energies close to the vortex core. As we will demonstrate, the corresponding length scales may be identified, in a first approximation, as the penetration length λ and the coherence length ξ. The peak amplitude variation, together with the Doppler shift energy, give the profile of the supercurrent intensity as a function of distance from the vortex center. By solving the London equation, a quantitative fit yields the values of both ξ and λ.

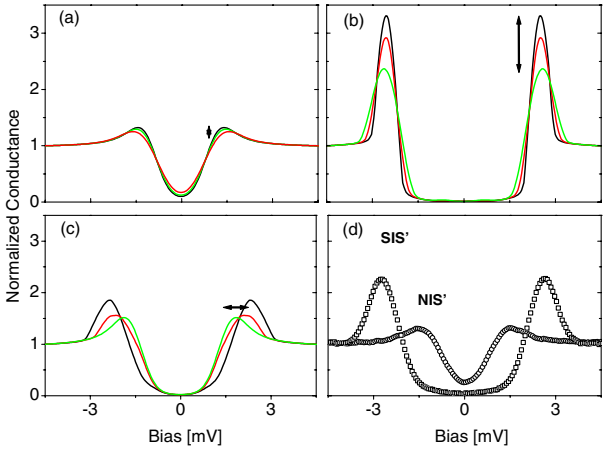

FIG. 1 (color online). Calculated tunneling conductance: (a) NIS′: normal metal tip with a SC sample, $\Delta = 1$ meV, $T = 2.3$ K, Doppler energy: 0 (highest peak), 0.3, 0.5 meV. (b) as in (a) but in the SIS′ configuration, with a SC tip $\Delta_{tip} = 1.5$ meV. (c) SIS′ with large Doppler shift = 0.65 meV and varying local sample gap $\Delta_{sample} = 0.6$ (widest gap), 0.3, 0 meV [24]. (d) Experimental tunnel conductance at $T = 2.3$ K for a $NbSe_2$ sample with a Nb tip (SIS′) and a normal Pt/Ir tip (NIS′). The SIS′ spectra appear more rounded than the calculated ones (b) due to the spread of gap values in $NbSe_2$ [19].

$NbSe_2$ crystals, grown using the Iodine Vapor Transport technique [17], were studied using a homemade UHV STM setup with a 2 K minimum temperature and a magnetic field up to 6 T [18]. The preparation and characterization of our Nb tips is reported in [16]. As a simple check, we first measured the spectra of the $NbSe_2$ sample in zero field, and at $T = 2$ K [see Fig. 1(d)]. These exhibit the typical features of a SIS junction: sharp symmetric peaks appear at the voltages $\pm(\Delta_{tip} + \Delta_{sample})/e$, with no particle-hole asymmetry seen. For comparison, we show the spectrum using a normal Pt/Ir tip (NIS junction). We thus obtain $\Delta_{Nb} = 1.5$ meV and $\Delta_{NbSe_2} = 1.0$ meV, in agreement with their bulk values.

We first describe the principles of STS vortex imaging with a SC tip. Figure 2 shows a typical result of a 330×330 nm^2 scan of the sample surface at $T = 4.5$ K and in a field of 0.06 T. At each point of a 256×256 point topographic image, a complete $I(V)$ tunneling spectrum was acquired in a bias range -10 mV to $+10$ mV. The conductance spectra, $dI/dV(V)$, were directly derived from *raw* $I(V)$ data. In Fig. 2(a) we present 8 selected conduc-

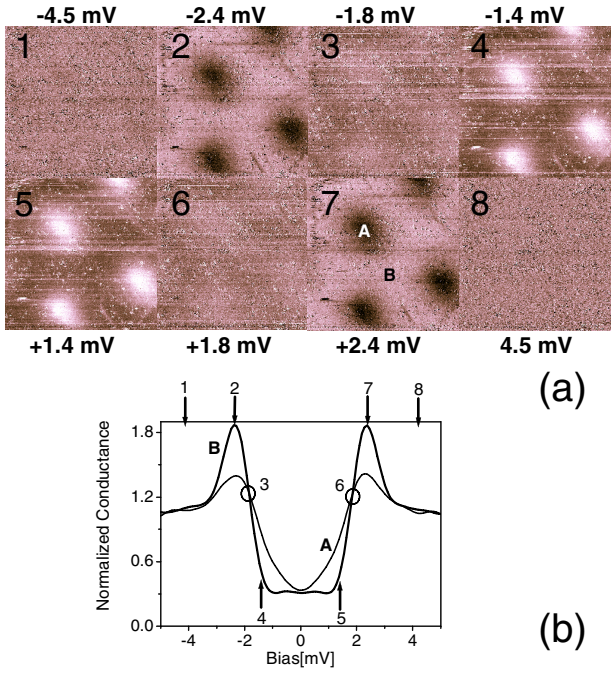

FIG. 2 (color online). (a) Fixed scale conductance maps (bias voltages indicated in the figure) of the vortex lattice, applied field 0.06 T, 330 nm × 330 nm area, $T = 4.5$ K. Strongest contrast is obtained at $V = \pm(\Delta_{Nb} + \Delta_{NbSe_2})/e$, maps 2 and 7, and at $V = \pm\Delta_{Nb}/e$, maps 4 and 5. (b) Local conductance measured in the vortex core, pos. A (NIS′) and at the exact center between the vortices, pos. B (SIS′). Arrows mark the selected voltages for the conductance maps (a).

tance maps. The maps are displayed in a *fixed* gray scale without any additional contrast treatment. Maps Nos. 2, 4, 5, and 7 show that the familiar triangular vortex lattice is successfully revealed by STS with a SC tip. Here, the intervortex distance of 190 nm matches the theoretical value $d = (2\phi_0/\sqrt{3}B)^{1/2} \simeq 200$ nm, for $B = 0.06$ T. First, contrary to the case of STS with a non-SC tip, the vortices do not appear in the maps near zero bias but rather at higher bias values. The maximum contrast is achieved at $eV \simeq \Delta_{tip}$ and $eV \simeq \Delta_{tip} + \Delta_{sample}$. Second, one observes an almost perfect symmetry of the contrast with respect to the Fermi level. Indeed, map No. 2 taken at -2.4 mV is almost identical to No. 7 obtained at $+2.4$ mV. In both, the vortices appear black due to the lower tunneling conductance in the vortex cores. Maps Nos. 4 and 5, taken at -1.4 mV and $+1.4$ mV, respectively, are also almost identical, but the vortices as the regions of higher conductance appear in white.

The origin of the map contrast is better understood from the spectra plotted in Fig. 2(b). The first, obtained in the center of the vortex, $\sigma_{NIS'}(V)$, shows the NIS shape, while the second, $\sigma_{SIS'}(V)$, taken at a point in between the vortices, shows the SIS one. At voltages above $(\Delta_{tip} + \Delta_{sample})/e$, V_8, $\sigma_{NIS'}(V) = \sigma_{SIS'}(V)$ and no contrast is observed. For lower V, $\sigma_{NIS'}(V) < \sigma_{SIS'}(V)$ with a maximum contrast achieved at $eV \simeq \Delta_{tip} + \Delta_{sample}$, V_7. The two spectra then cross, V_6. Following $\sigma_{SIS'} < \sigma_{NIS'}$ and a second high but inverted contrast is found for $eV \simeq \Delta_{tip}$, V_5. Finally at $V = 0$, $\sigma_{SIS'} \simeq \sigma_{NIS'}$: the contrast is negligible. Qualitatively, features in the sample DOS, besides being enhanced, are shifted in energy by an amount Δ_{tip}. By selecting the sharpest positive and negative maps we determine, from the STS: $\Delta_{Nb} = 1.4$ meV and $\Delta_{NbSe_2} = 1.0$ meV.

To study the superfluid profile, we focused on a single vortex lattice unit cell and reduced the temperature to 2.3 K, improving spatial and energy resolutions. A low field (0.05 T) was applied minimizing supercurrent overlap from adjacent vortices. Figure 3 shows conductance maps at three selected voltages. The apparent vortex size and shape depend sensitively on the particular bias: Map (a), obtained at the SIS peak, $eV \simeq \Delta_{tip} + \Delta_{sample}$, shows a much larger diameter than map (c), obtained at $eV \simeq \Delta_{tip}$, revealing essentially the vortex core. Such enlargement is precisely due to the Doppler effect of the screening currents. Map (b), obtained at the SIS/SIN crossing point [V_6 in Fig. 2(b)] where little contrast was expected, reveals a star-shaped halo.

Figure 4 shows the change in the spectra as a function of distance from the vortex center. As a first approximation, we can neglect the very small angular anisotropy seen only in Fig. 3(b). To reduce the noise, the spectra were averaged over a circle of radius r, concentric with the vortex. In between the vortices the dI/dV curve (A) shows the typical SIS shape. Approaching the vortex, the peak amplitude

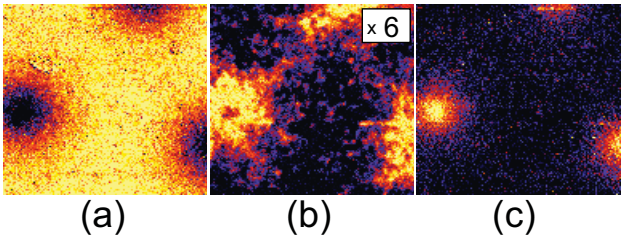

FIG. 3 (color). Conductance maps of a 210×210 nm^2 area, $T = 2.3$ K, applied field 0.05 T. Maps selected at voltages: $V = 2.6$ mV, 2.2 mV, and 1.6 mV corresponding to (a) the SIS′ peak, (b) the SIS′/NIS′ intersection point and (c) the NIS′ peak. These emphasize: (a) long range variations in the SIS′ peak height, (b) weak angular anisotropy, and (c) vortex core. For visibility the contrast in (b) was enhanced by a factor of 6.

drops dramatically (red spectra in Fig. 4) as expected from the calculations [Fig. 1(b)]. Close to the vortex the main effect is a shift of the gap-edge peak to lower voltages (black spectra in Fig. 4), similar to the shift shown in Fig. 1(c). At the vortex core (B) we observe an additional dip-hump features (D, H) with a slight increase of the gap-edge peak amplitude. The effect is the signature of the vortex core states which exist near the Fermi energy, but are shifted to a voltage above Δ_{tip}/e in our case.

Figure 5 summarizes the prominent changes in the spectra in plots of the peak position and amplitude as a function of distance r from the core. Starting at large r, the peak height, initially at 2.4, is continuously diminished, finally leveling off at a value ~ 1.5 at $r = r_c \simeq 110$ Å (dashed

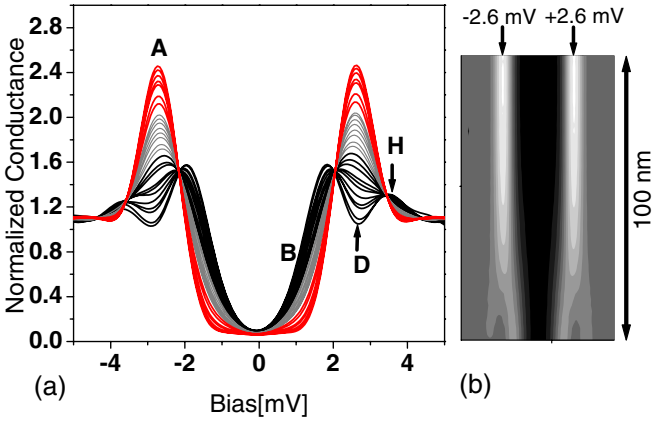

FIG. 4 (color online). (a) Evolution of the conductance spectra as a function of distance from the vortex center. Far from the vortex (A) the spectra show SIS features with high peaks at $(\Delta_{tip} + \Delta_{sample})/e$. The peak height is first lowered and then followed by a shift to a lower voltages, near $\simeq \Delta_{tip}/e$. Close to the vortex center (B) a dip-hump feature (D, H) and a slight increase in the peak height are observed due the core bound states. (b) Gray scale representation of the spectra shown in (a) as a function of bias (x axis) and distance form vortex center (y axis). The branching seen at the bottom of the image is the signature of the core bound states.

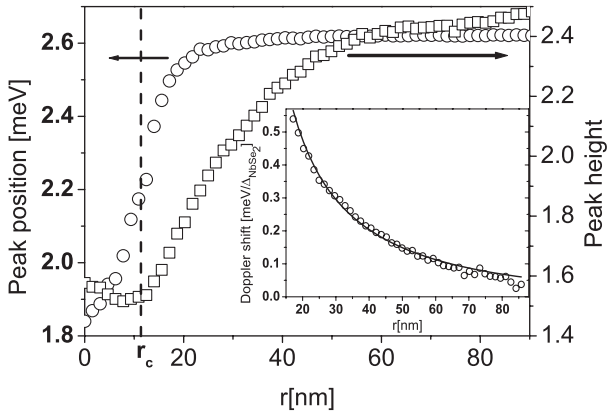

FIG. 5. Gap-edge peak energy (○) and amplitude (□) as a function of distance from the vortex center, r. Inset shows the Doppler shift energy, in units of Δ_{NbSe_2}, as a function of r (○). Solid line is a best fit of $\frac{\pi}{2}\frac{\xi}{\lambda}K_1(r/\lambda)$ obtained using $\lambda = 68$ nm and $\xi = 6.6$ nm.

line). This lowering of the peak amplitude is due to the increase in the superfluid velocity as one approaches the vortex core, which saturates at the critical velocity, $\mathbf{v} \simeq \mathbf{v}_c$ at $r \simeq r_c$. On the contrary, the peak *energy* is roughly constant (at ~2.6 meV) for all $r \gtrsim 2r_c$ but then decreases rapidly ($r \sim r_c$) down to its minimum value ~1.8 meV at $r = 0$. Thus, the peak position as a function of r, shifted downwards by $\sim\Delta_{\text{tip}}$, matches the PP profile. Using r_c to estimate $\sqrt{2}\xi$, we find $\xi \simeq 80$ Å and from the peak amplitude profile, $\lambda \simeq 750$ Å. In short, Fig. 5 gives a picture of the PP and supercurrent profiles of a vortex, of core radius r_c.

λ and ξ may also be extracted through the Doppler shift energy [from Eq. (1)] as a function of r (see inset of Fig. 5). We have fitted the data with the function: $\frac{\pi}{2}\frac{\xi}{\lambda}K_1(r/\lambda)$, derived from the London equation for an isolated vortex, where $K_1(x)$ is the modified Bessel function of order 1. (This approximation neglects Fermi surface and gap anisotropies.) The best fit is found using $\xi = 66$ Å and $\lambda = 680$ Å and is shown by a line in the inset. Finally, the Doppler shift at $r = \xi$, with the Fermi momentum $mv_F \simeq \hbar\pi/2a$, where $a \simeq 3.5$ Å is the lattice constant, leads to $v_c \approx 180\ \text{m s}^{-1}$.

In principle, our data could be perturbed by the magnetic field. Observing a nondistorted lattice proves that the interaction between the SC diamagnetic tip and the vortices is negligible. Zeeman splitting might also affect the DOS especially that of the tip. Curve B in Fig. 4, obtained at the vortex core (highest field), proves that the SC DOS of our Nb tips is unperturbed. Indeed, at the field used, the Zeeman energy, $2\mu_B H \sim 0.006$ meV, is negligible. This concords with our previous studies revealing a surprisingly weak effect of magnetic fields on Nb tips [16]. This is due to the tip's apex size being smaller than both ξ and λ with the critical field value depending on the exact tip geometry [16]. We note that the rounding of the conductance at voltages slightly below the peak (Fig. 4) is faster than the predicted one [Fig. 1(b)]. We attribute this to the gap distribution (0.4 meV–1.3 meV) found in $NbSe_2$ [19–21]. Lacking a theory for the possible effect of currents in such a case, our results merely indicate that the low end of the gap distribution is diminished faster by the currents, in agreement with the models of [22,23].

In conclusion, we have presented detailed STS mapping of the vortex lattice using a SC tip. The main result is the enhanced sensitivity to the Doppler shift, allowing a detailed nanometer scale mapping of the pair currents in any SC sample. It could then be applied to cases where there is an external current source, an oblique magnetic field, or to confined superconductors, where the supercurrent distribution is unknown.

Sample preparation was supported by the NCCR research pool MaNEP of the Swiss NSF.

[1] A. A. Abrikosov, Sov. Phys. JETP **5**, 1174 (1957).
[2] C. Caroli *et al.*, Phys. Lett. **9**, 307 (1964).
[3] H. F. Hess *et al.*, Phys. Rev. Lett. **62**, 214 (1989).
[4] H. F. Hess *et al.*, Phys. Rev. Lett. **64**, 2711 (1990).
[5] Ch. Renner *et al.*, Phys. Rev. Lett. **67**, 1650 (1991).
[6] S. H. Pan *et al.*, Phys. Rev. Lett. **85**, 1536 (2000).
[7] P. Fulde, *Tunneling Phenomena is Solids* (Plenum, New York, 1969), p. 427.
[8] A. Anthore *et al.*, Phys. Rev. Lett. **90**, 127001 (2003).
[9] For a thorough review see: P. Björsson, Ph.D. Thesis, Stanford University, 2005, and references therein.
[10] J. Ngai *et al.*, Phys. Rev. B **72**, 054513 (2005).
[11] T. Dahm *et al.*, Phys. Rev. B **66**, 144515 (2002).
[12] S. H. Pan *et al.*, Appl. Phys. Lett. **73**, 2992 (1998).
[13] O. Naaman *et al.*, Rev. Sci. Instrum. **72**, 1688 (2001).
[14] H. Suderow *et al.*, Physica (Amsterdam) **369C**, 106 (2002).
[15] F. Giubileo *et al.*, Phys. Rev. Lett. **87**, 177008 (2001).
[16] A. Kohen *et al.*, Physica (Amsterdam) **419C**, 18 (2005).
[17] R. Bel *et al.*, Phys. Rev. Lett. **91**, 066602 (2003).
[18] T. Cren *et al.*, Europhys. Lett. **54**, 84 (2001).
[19] J. G. Rodrigo and S. Vieira, Physica (Amsterdam) **404C**, 306 (2004).
[20] T. Yokoya *et al.*, Science **294**, 2518 (2001).
[21] E. Boaknin *et al.*, Phys. Rev. Lett. **90**, 117003 (2003).
[22] D. Zhang *et al.*, Phys. Rev. B **70**, 172508 (2004).
[23] E. J. Nicol and J. P. Carbotte, Phys. Rev. B **72**, 014520 (2005).
[24] The conductance curves were convoluted with a Gaussian of width 0.4 mV matching our bias jitter.